



PAPER

## Mechanical properties of TPDH-graphene: atomistic aspect

To cite this article: Qing Peng *et al* 2024 *Phys. Scr.* **99** 115996

View the [article online](#) for updates and enhancements.


### You may also like

- [Application of fractional modified taylor wavelets in the dynamical analysis of fractional electrical circuits under generalized caputo fractional derivative](#)  
Ashish Rayal, Monika Anand and V K Srivastava
- [Image encryption algorithm based on matrix projective combination-combination synchronization of an 11-dimensional time delayed hyperchaotic system](#)  
Jyotsna Kumari Bharti, P Balasubramaniam and K Murugesan
- [Laser modulation to plateau region and intensity of high-order harmonic generation in monolayer MoTe<sub>2</sub>](#)  
Zhiqiang Ji, Chenglong Wu, Xiaoyu Liu et al.



## PAPER

## Mechanical properties of TPDH-graphene: atomistic aspect

RECEIVED  
13 March 2024REVISED  
3 October 2024ACCEPTED FOR PUBLICATION  
16 October 2024PUBLISHED  
28 October 2024Qing Peng<sup>1,2,3,\*</sup> , Gen Chen<sup>2,4,5</sup>, Zeyu Huang<sup>2,4,5</sup>, Yuqiang Zhang<sup>4,5</sup>, Xiaofan Zhang<sup>2,6</sup>, Xiao-Jia Chen<sup>1,\*</sup> and Zhongwei Hu<sup>4,5,\*</sup><sup>1</sup> School of Science, Harbin Institute of Technology, Shenzhen 518055, People's Republic of China<sup>2</sup> State Key Laboratory of Nonlinear Mechanics, Institute of Mechanics, Chinese Academy of Sciences, Beijing 100190, People's Republic of China<sup>3</sup> Guangdong Aerospace Research Academy, Guangzhou 511458, People's Republic of China<sup>4</sup> Institute of Manufacturing Engineering, Huaqiao University, Xiamen 361021, People's Republic of China<sup>5</sup> Institute of Mechanical Engineering and Automation, Huaqiao University, Xiamen 361021, People's Republic of China<sup>6</sup> College of Aerospace Engineering, Chongqing University, Chongqing 400044, People's Republic of China

\* Authors to whom any correspondence should be addressed.

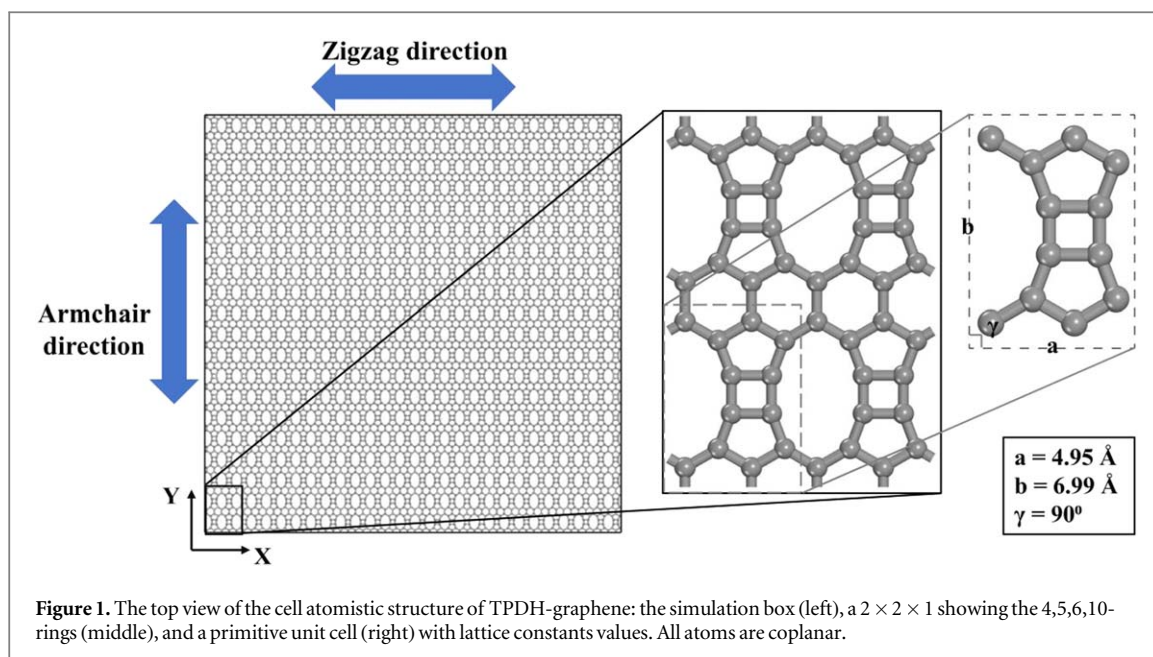
E-mail: [pengqing@imech.ac.cn](mailto:pengqing@imech.ac.cn), [xjchen@hit.edu.cn](mailto:xjchen@hit.edu.cn) and [huzhongwei@hqu.edu.cn](mailto:huzhongwei@hqu.edu.cn)**Keywords:** TPDH-graphene, MD, mechanical property, defectsSupplementary material for this article is available [online](#)**Abstract**

TPDH-graphene is a new type of two-dimensional carbon material predicted by first-principles calculations to have tetragonal (T), pentagonal (P), decagonal (D) and hexagonal (H) carbon ring structures. First-principles calculations show that this special structure gives it excellent mechanical properties and promising applications in nanoelectronics. In this paper, a comprehensive test of its mechanical properties was carried out using the classical molecular dynamics (MD), mainly exploring the effects of factors such as tensile direction and temperature on its mechanical properties, and exploring the effects of introducing rectangular and circular defects on its mechanical properties. The results show that: TPDH-graphene exhibits significant anisotropy in zigzag and armchair directions, and the material exhibits some tensile toughness in armchair direction; the mechanical properties of the material are weakened at higher temperatures; the adding of defects leads to the reduction of the mechanical properties of the material in different directions to different degrees, and the The tensile toughness in the armchair direction is weakened by the addition of defects.

**1. Introduction**

Graphene is a typical two-dimensional carbon material that has received a lot of attention since it was proposed in 2004, with applications in fields such as electrode materials and electronics [1–3]. Excellent mechanical properties due to graphene's special honeycomb structure [4–7], Studies of the mechanical properties of two-dimensional graphene have revealed significant anisotropy [8–11]; The researchers also investigated the effects of temperature and strain rate on the mechanical properties of graphene, showing that higher temperatures cause the material to soften, leading to a decrease in mechanical properties including bulk modulus, tensile strength, fracture toughness, while stretching at high strain rates results in the material exhibiting higher tensile strength and strain at break [12–16]; The effect of defects on the mechanical properties of 2D graphene was also investigated, and the results showed that the mechanical properties of graphene are usually weakened to varying degrees when defects are taken into account [17–23].

The existence of similar 2D carbon materials with mechanical properties similar to graphene is of great interest to researchers, and with the development of computer computing power, researchers have used first-principles methods to predict the structure of some 2D carbon materials with good properties [24–29]. In 2021, a new 2D carbon material called TPDH-graphene has been proposed for the first time, with excellent physical properties including dynamic and thermal stability, the ability to absorb UV light in specific areas and its unusual current regulation behaviour based on first principles calculations and has promising applications in



nano-electronics [30]. Subsequent researchers have investigated the kinetics and electronic structure of TPDH-graphene in the hydrogenation mode [31].

TPDH-graphene is a predicted new two-dimensional carbon material, and its preparation is still facing challenges, so it is difficult to measure its mechanical properties through experimental methods. However, molecular dynamics methods can help us study their mechanical properties, and the results obtained will deepen our understanding of the mechanical properties of this new material, which will help speed up the design of new two-dimensional carbon materials, preparation and final application. In this paper we use MD to make a comprehensive test on its tensile mechanical properties, including the strain rates, direction of stretching (the zigzag and armchair directions of stretching indicated by blue arrows in figure 1), temperature, and consider the effect of defects on its mechanical properties, which will provide a reference for the practical application of the material in the later stage.

## 2. Materials and methods

As shown in figure 1, the lattice constants of TPDH-graphene are  $a = 4.95 \text{ \AA}$ ,  $b = 6.99 \text{ \AA}$ , and  $\gamma = 90^\circ$ , and the bond lengths of the C–C bonds are  $1.41 \text{ \AA}$ ,  $1.44 \text{ \AA}$ , and  $1.5 \text{ \AA}$ , and it consists of a four-membered ring, a five-membered ring, a six-membered ring, and a ten-membered ring, it belongs to the space group of Pmmm(47) [30]; A simulation model of a single layer of TPDH-graphene was developed, the thickness of the single layer was taken to be  $3.34 \text{ \AA}$ , the time step was  $0.0001 \text{ ps}$ . The tensile simulation was performed using a single layer of TPDH-graphene which is ideal with any defects. The simulation box is approximately  $14 \text{ nm} \times 14 \text{ nm} \times 10 \text{ nm}$ , containing 6720 atoms and the size effect will be investigated in the next section; To ensure the accuracy of the results, a single layer of TPDH-graphene ( $30 \text{ nm} \times 30 \text{ nm} \times 10 \text{ nm}$ ) containing 30960 atoms is used in the tensile simulation considering the effect of defects. The TPDH-graphene structure contains six-membered rings of carbon atoms, and based on its structural features, we defined two tensile orientations, the one is along the zigzag direction (parallel to the X direction), the other is armchair direction which is parallel to the Y direction. We mainly investigated the mechanical properties of TPDH-graphene in the zigzag and armchair directions based on the structural characteristics of TPDH-graphene.

In the simulations to study the effect of system size and boundary, mechanical properties and the effect of defects, the temperature was maintained at  $300 \text{ K}$ , the strain rate was set to  $0.001 \text{ ps}^{-1}$  and the pressure was set to  $0 \text{ Pa}$ . We used molecular dynamics simulations and the open source software LAMMPS [32], and processed the results of the molecular dynamics simulations with the visualisation tool OVITO [33]. Tersoff potential function has been successfully applied to the testing of the mechanical properties of graphene [16, 34–42]. Based on the basic Tersoff potential function, some researchers have modified the parameters of the potential function to better apply to the simulation of carbon materials, and achieved good results [16, 19, 42, 43]. In this study, the Tersoff potential function is applied to simulate the interaction between carbon atoms in TPDH-graphene [44]. It is important to note that no experimental data on TPDH-graphene are currently available, and therefore the

Tersoff potential function is not necessarily the most appropriate potential function to apply to TPDH-graphene simulations. We describe our exploration of the choice of potential function in the Supplementary Document.

The Tersoff potential function is a three-body potential that provides a good description of covalent bonding interactions in materials. The total potential energy of the Tersoff potential function can be written as the sum of the potential energies of  $N$  atoms:

$$E = \frac{1}{2} \sum_{i \neq j}^N f_c(r_{ij} + \delta) [f_R(r_{ij} + \delta) + b_{ij} f_A(r_{ij} + \delta)] \quad (1)$$

Here,  $f_c(r_{ij})$ - truncation function;  $f_R(r_{ij})$ - repulsion term between atoms  $i$  and  $j$ ;  $f_A(r_{ij})$  - attraction term between atoms  $i$  and  $j$ ;  $b_{ij}$ - bonding bond order between atoms  $i$  and  $j$ .

The mathematical form of the truncated function is as follows:

$$f_c(r_{ij}) = \begin{cases} 1 & r_{ij} < R - D \\ \frac{1}{2} \left[ 1 - \sin\left(\frac{\pi}{2} \cdot \frac{r_{ij} - R}{D}\right) \right] & R - D < r_{ij} < R + D \\ 0 & r_{ij} > R + D \end{cases} \quad (2)$$

Here,  $R-D$  and  $R+D$  are the inner and outer truncation radii.

$R$  and  $D$  are the two fitting parameters in the Tersoff potential function. In our work,  $R = 1.95 \text{ \AA}$  and  $D = 0.15 \text{ \AA}$ , which is consistent with the parameters in the paper [44].

Griffith's theory suggests that brittle fracture of a material is due to localised stress concentrations caused by crack defects inherent in the material, and that the fracture stress of a brittle material is closely related to the length of the crack [45], which takes the form of a mathematical equation (3):

$$\sigma_f = \sqrt{\frac{2E\gamma_s}{\pi a}} \quad (3)$$

Here,  $\gamma_s$  - surface free energy;  $E$  - Young's modulus;  $a$  - crack length.

Based on Griffith's theory, Zhao proposed an analytical expression for the existence of the fracture strength of graphene under uniaxial stretching concerning temperature and strain rate [12], which has been applied to the study of fracture of 2D graphene [46].

In this paper, the stresses and strains in two-dimensional carbon materials during uniaxial stretching are calculated. The strain is calculated as shown in equation (4):

$$\varepsilon = \frac{l_f - l_i}{l_i} \quad (4)$$

Here,  $l_f$  - final length of 2D carbon material sheet;  $l_i$  - initial length of 2D carbon material sheet.

The stress is calculated as shown in equation (5):

$$\sigma = P_i \frac{l_z}{h_0} = \frac{F_i}{l_j l_z} \cdot \frac{l_z}{h_0} \quad (5)$$

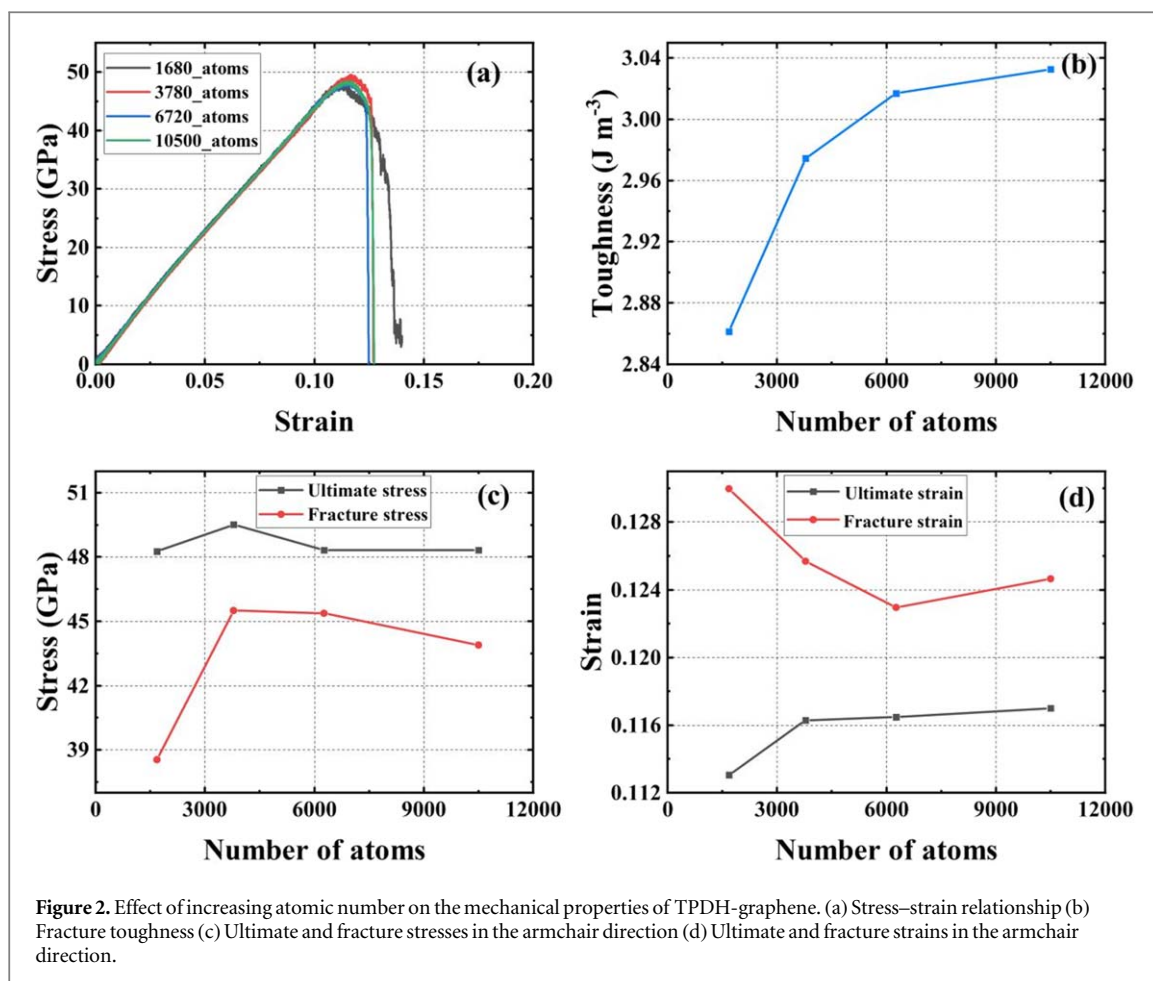
Here,  $P_i$  - the stress component of the box in a given direction;  $l_z$  - length of the box in the  $z$ -direction;  $h_0$  - the layer thickness of graphene, here we take  $3.34 \text{ \AA}$ ;  $F_i$  - the force on the box in a given direction;  $l_j$  - the length of a 2D carbon material which is perpendicular to the direction of stretching.

For a given layer thickness of  $3.34 \text{ \AA}$ , this is actually an important parameter to consider when calculating tensile stresses. For this predicted new 2D carbon material structure we had difficulty determining its single layer thickness, so we used the layer thickness of graphene to approximate it, which has been widely used in similar research work [23, 47]. In terms of data collection, we use the data output command that comes with the LAMMPS software, which helps us to record the output data for each time step and average it every 250 time steps.

## 3. Results and discussions

### 3.1. Effects of system size and boundary

Choosing a model with the right number of atoms is crucial in balancing the accuracy of the calculation results and reducing the amount of computation. Too small a number of atoms in the system makes it difficult to describe the mechanical behaviour of the system correctly, and too many atoms in the system consumes unnecessary computational resources. Therefore, we have the effect of the number of atoms on the mechanical properties of TPDH-graphene.



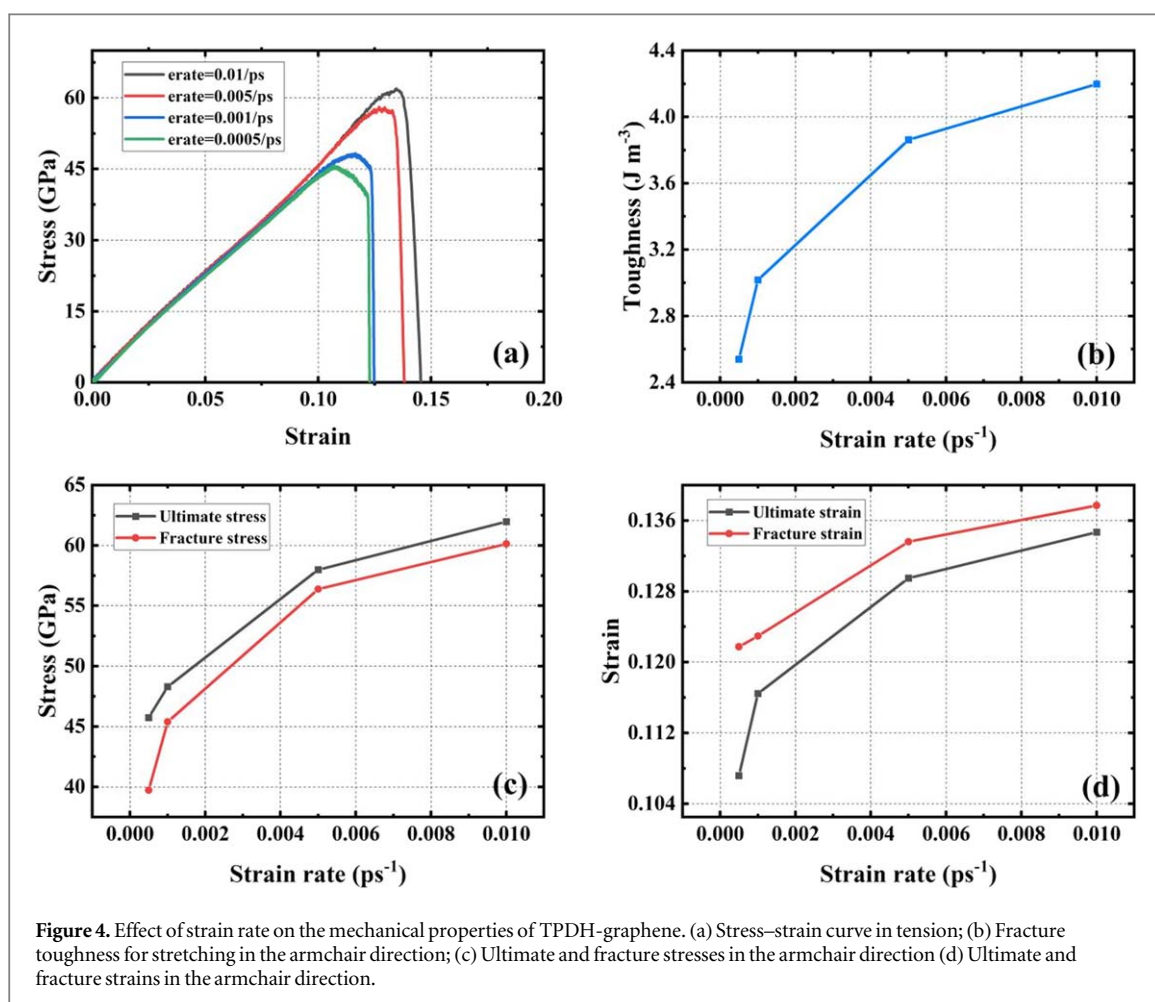
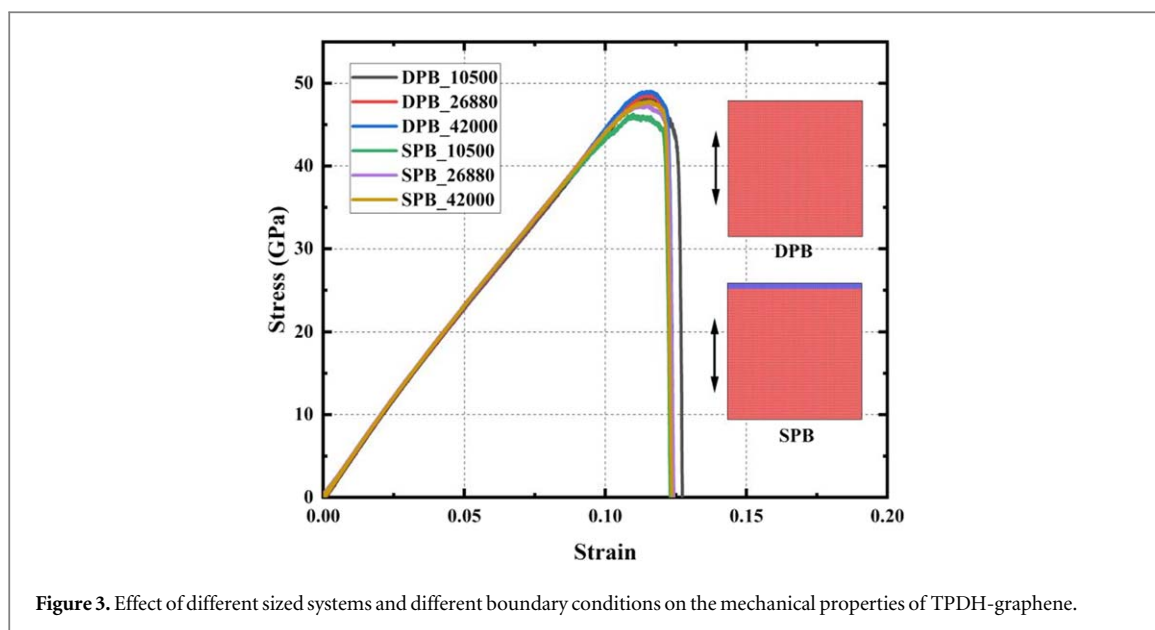
The results of the tensile test along the armchair direction are shown in figure 2(a), which shows that the stress–strain curves become smooth as the number of atoms in the system increases and the differences between them gradually decrease and that the system of 1680 atoms describes the mechanical behaviour of the material with poor accuracy. We investigated the effect of the number of atoms of the system on the fracture toughness, as shown in figure 2(b). The change in the value of fracture toughness flattens with the increasing number of atoms contained in the system. Furthermore, changes in the values of ultimate stress–strain and fracture stress–strain flatten out as the number of atoms contained in the system increases. As shown in figures 2(c) and (d), TPDH-graphene containing 1670 carbon atoms has the largest difference between ultimate stress–strain and stress–strain at break for uniaxial stretching in the armchair direction, and the difference decreases with the increase in the number of carbon atoms.

The effects of model boundary conditions and model size on the simulation results are further discussed. As shown in figure 3, the three sizes of the studied systems set up contain 10500 (18 × 18 nm), 26880 (28 × 28 nm), and 42000 (35 × 35 nm) carbon atoms, and the boundary conditions are set up in the plane with double periodicity (DPB) and single periodicity (SPB), respectively. SPB is achieved by fixing the carbon atoms at the edges [48]. In the large system containing 42000 carbon atoms, the ultimate stress of SPB is reduced by 2.55% compared with that of DPB, and the ultimate strain remains the same. From the simulation results, it can be seen that both the boundary conditions of the model and the size of the system have limited effects on the simulation results.

It is difficult to accurately describe the mechanical behaviour of TPDH-graphene with too few atoms of the system, and further increasing the number of atoms has a limited effect on the mechanical properties of TPDH-graphene, so we selected 6720 atoms for the study. The boundary conditions of the model are set to DPB.

### 3.2. Effects of strain rate

Strain rate has a significant effect on the mechanical properties of materials [21]. To investigate the effect of strain rate on the mechanical properties of TPDH-graphene, the temperature was kept constant at 300 K, the pressure was kept constant at 0 Pa and tensile tests were carried out in the armchair direction. The results are shown in figure 4, the strain rate increased from 0.0005 to 0.01 ps<sup>-1</sup>, i.e., an increase of two orders of magnitude, and the stress at fracture, strain at fracture and fracture toughness decreased by 33.92%, 11.62% and 39.51%,



respectively. The ultimate stress was reduced by 26.17% and the ultimate strain by 20.44%. As shown in figures 4(c) and (d), the material exhibits tensile toughness for the stretching of TPDH-graphene in the armchair direction at different strain rates.

We have observed that increasing the strain rate causes TPDH-graphene to exhibit stronger mechanical properties in the tensile test, which is due to the shorter response time of the material to load at high strain rate. Lower strain rates, on the other hand, allow more time for the atoms to thermally vibrate, which increases the

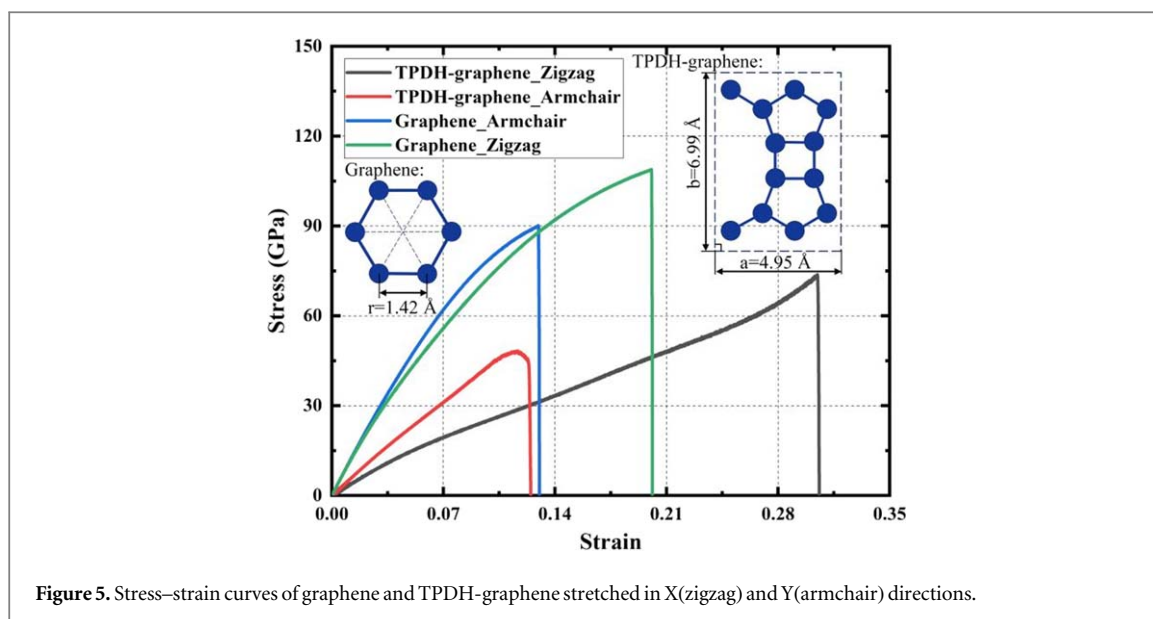


Figure 5. Stress–strain curves of graphene and TPDH-graphene stretched in X(zigzag) and Y(armchair) directions.

Table 1. Mechanical properties of TPDH-graphene in zigzag and armchair directions.

Tensile direction	Ultimate stress (GPa)	Ultimate strain	Fracture stress (GPa)	Fracture strain	Toughness ( $\text{J m}^{-3}$ )
Along zigzag	73.75	0.3046	73.12	0.3049	11.0
Along armchair	48.31	0.1165	45.39	0.1229	3.02

probability that the atoms will overcome the energy barrier and break the C–C bond. This is similar to previous researchers who studied the effect of strain rate on the fracture strength of graphyne [49–51].

### 3.3. Mechanical properties

#### 3.3.1. Mechanical properties in different directions

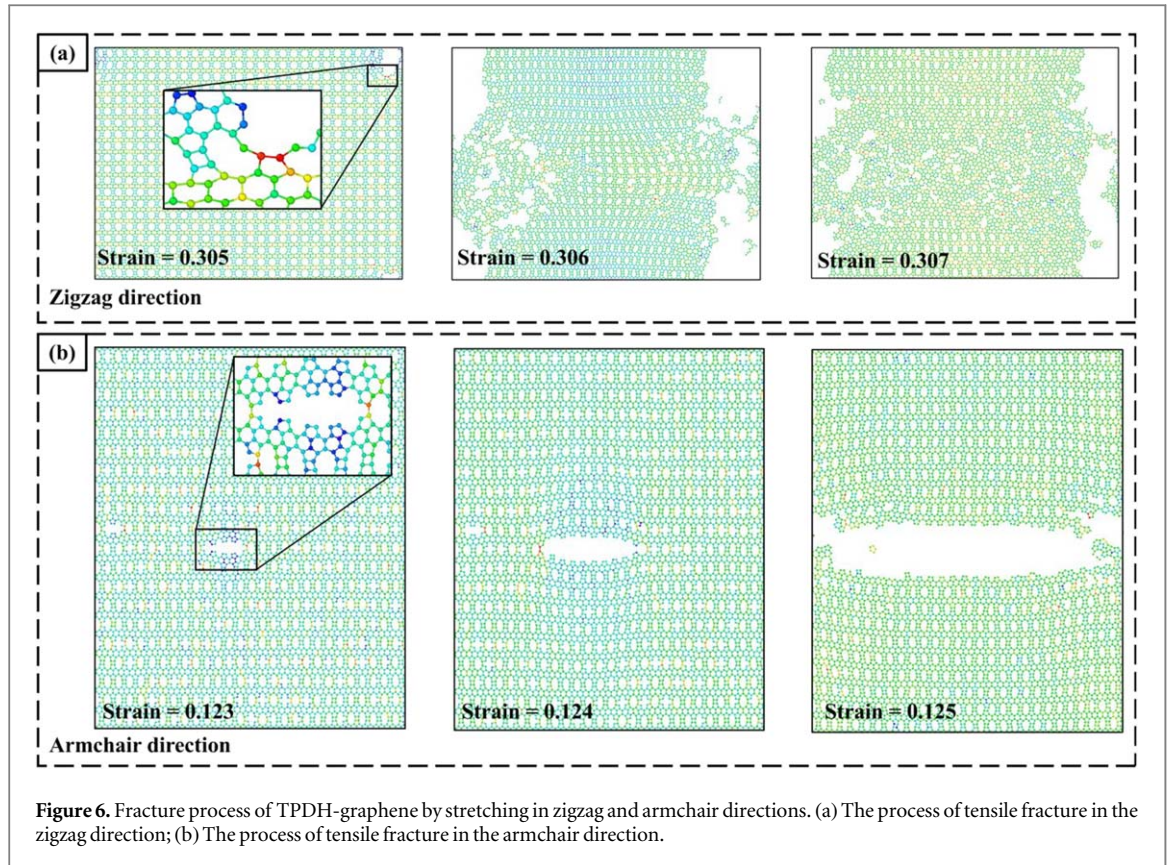
Figure 5 shows the stress–strain curves of the tensile tests performed on TPDH-graphene in the  $x$ (zigzag) and  $y$ (armchair) directions, respectively, and the structural variability results in it exhibiting significant variability in its stress–strain curves under different loading directions.

Table 1 shows the mechanical properties of TPDH-graphene in tensile tests in both directions, the ultimate strength in zigzag and armchair direction is 73.75 GPa and 48.31 GPa, respectively, which is 52.66% higher in zigzag direction compared to armchair direction. The ultimate strain in zigzag and armchair direction is 0.305 and 0.116, respectively, which is 162.93% higher in zigzag direction compared to armchair direction. The fracture toughness in zigzag and armchair direction is 11.019 and 3.016, respectively, which is 265.35% higher in zigzag direction compared to armchair direction.

Ultimate stress is the maximum stress in the tensile stress–strain curve and the corresponding strain is the ultimate tensile stress as the same as the conventional deformation. The Fracture stress is the stress value in the tensile stress–strain curve where the materials are failed into parts due to the tensile, and the corresponding strain is the fracture strain. Furthermore, from the tensile results of TPDH-graphene in both directions, the fracture along the zigzag direction was brittle, while the fracture along the armchair direction exhibited a certain degree of tensile toughness. The fracture stress for stretching along the armchair direction decreased by 6.06% compared to the ultimate stress limit stress and the fracture strain increased by 5.56% compared to the ultimate strain.

The form of tensile fracture in the zigzag direction is shown in figure 6(a), starting from a strain of 0.305, with cracks appearing from both sides, spreading towards the centre and finally breaking completely. Armchair direction is shown in figure 6(b), starting from a strain of 0.123, with cracks appearing from the centre, spreading towards both sides and finally breaking completely.

We compared the mechanical properties of TPDH-graphene with 2D graphene. The simulation of the uniaxial tensile test of graphene was carried out using the AIREBO potential function with the cut-off radius of the potential set to 2.0, and the obtained results of the uniaxial tensile test of the 2D graphene are in agreement with the conclusions of the previous studies [10, 43]. The mechanical properties of TPDH-graphene are



**Figure 6.** Fracture process of TPDH-graphene by stretching in zigzag and armchair directions. (a) The process of tensile fracture in the zigzag direction; (b) The process of tensile fracture in the armchair direction.

significantly weaker than those of graphene, while exhibiting significant anisotropy. This paper calculates the surface densities of both materials and also the line densities of TPDH graphene along the zigzag and armchair directions. The formula for calculating the surface density of the two-dimensional carbon material is shown in equation (6):

$$\rho_{Surface} = \frac{m}{S} \quad (6)$$

Here,  $m$ -the total mass of the atoms;  $S$ -the projected area of the two-dimensional material in the plane.

The formulae for calculating the projected line density of 2D carbon materials are shown in equation (7):

$$\rho_{Linear} = l \times \rho_{Surface} \quad (7)$$

Here,  $l$ -the projected length of the 2D carbon material along a certain direction.

Through the above calculation, the surface density of graphene is  $\rho_{Graphene} = 7.66 \times 10^{-7} \text{ Kg/m}^2$ , and that of TPDH-graphene is  $\rho_{TPDH-graphene} = 6.91 \times 10^{-7} \text{ Kg/m}^2$ , which is reflected in the stress-strain curves of uniaxial stretching as the mechanical properties of graphene are better than those of TPDH-graphene. The projected line densities of TPDH-graphene along the two directions are  $\rho_{Armchair} = 3.42 \times 10^{-16} \text{ Kg/m}$  and  $\rho_{Zigzag} = 4.83 \times 10^{-16} \text{ Kg/m}$ , respectively. TPDH-graphene has a bigger mass density of carbon atoms along the zigzag direction compared to the armchair direction, so the material shows significant anisotropy in uniaxial tensile tests and possesses stronger mechanical properties along the zigzag direction.

Based on simulation results and theoretical analysis, it is believed that the existence of differences in mechanical properties in the zigzag and armchair directions is due to the structural differences of TPDH-graphene in different directions. The arrangement of four-membered, five-membered, six-membered and ten-membered rings in both directions leads to different projected line density of carbon atoms in zigzag and armchair directions. Furthermore, by observing the fracture process of TPDH-graphene, it can be found that uniaxial stretching along the armchair direction breaks the four-membered carbon ring to form a crack and further extends along the arrangement of the four-membered carbon ring; whereas uniaxial stretching along the zigzag direction needs to complete the destruction of the five-membered and six-membered carbon rings in the initial stage of the disruption of the material. The stability of the mechanical properties of the four carbon rings is different. It is mainly due to the differences in the projected linear densities of the carbon atoms and the differences in the structural stability of the four carbon rings that differ leading to the significant anisotropy exhibited in the mechanical properties of TPDH-graphene.

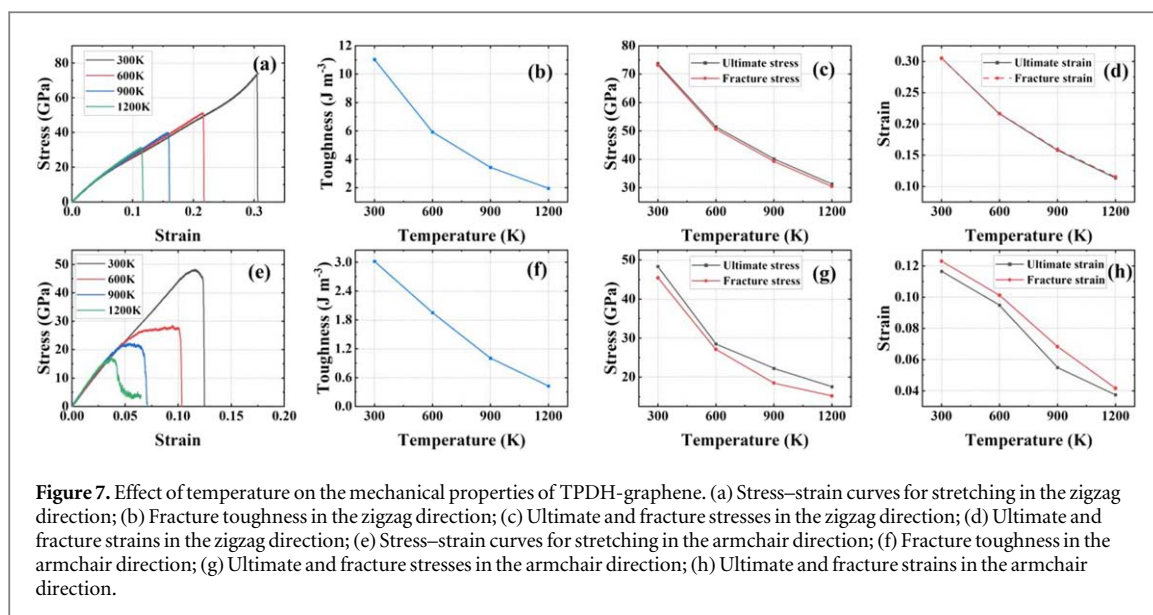


**Figure 7.** Effect of temperature on the mechanical properties of TPDH-graphene. (a) Stress–strain curves for stretching in the zigzag direction; (b) Fracture toughness in the zigzag direction; (c) Ultimate and fracture stresses in the zigzag direction; (d) Ultimate and fracture strains in the zigzag direction; (e) Stress–strain curves for stretching in the armchair direction; (f) Fracture toughness in the armchair direction; (g) Ultimate and fracture stresses in the armchair direction; (h) Ultimate and fracture strains in the armchair direction.

### 3.3.2. Mechanical properties at different temperatures

The effect of temperature on the mechanical properties of the material is significant [47, 51, 52]. In order to investigate the effect of temperature on the mechanical properties of TPDH-graphene, the strain rate was kept constant at 0.001 ps<sup>-1</sup>, the pressure was kept constant at 0 Pa and four temperatures, 300 K, 600 K, 900 K and 1200 K, were selected for tensile tests in zigzag and armchair directions, respectively. As shown in figures 7(a) and (e), the stress–strain behaviour of TPDH-graphene in zigzag and armchair directions decreases with increasing temperature. The corresponding fracture stresses and strains in both directions decrease with increasing temperature as shown in figures 7(c), (d), (g) and (h). In addition, the fracture toughness in the zigzag and armchair directions gradually decreases with increasing temperature as shown in figures 7(b) and (f).

It can be concluded that high temperature causes softening of the material and higher temperature decreases the mechanical properties of TPDH-graphene, which is consistent with the effect of temperature on the mechanical properties of graphene [4, 12, 53].

In addition, it is worth noting that as the temperature increases, the tensile of TPDH-graphene in the zigzag direction maintains brittle fracture, while the tensile in the armchair direction still exhibits tensile toughness. The results of the tensile tests of TPDH-graphene along the armchair direction at four temperatures of 300K, 600K, 900K and 1200K show that the fracture stress decreased by 6.06%, 4.87%, 16.97% and 13.17%, respectively, compared with the ultimate stress; the fracture strain increased by 5.56%, 6.61%, 24.38% and 11.36% respectively, compared with the ultimate strain.

### 3.4. Effects of defects

The absence of carbon atoms is a common form of defects in 2D carbon materials, which has a significant impact on the mechanical properties of materials [54–57]. Rectangular and circular defects are two forms of defects that are often studied [23, 58].

Figure 8 illustrates the setting of the defects and the energy stability of the system containing the defects. The defects set up in this paper are vacancy atom defects with certain geometrical shapes (rectangular defects and circular defects), and the use of the percentage of missing atoms provides a more detailed representation; the three rectangular defects are: 10 Å (0.09%), 15 Å (0.17%) and 30 Å (0.32%), and three circular defects: 10 Å (0.12%), 15 Å (0.20%) and 30 Å (0.81%); rectangular type I cracks are the most common form of cracks in materials undergoing fracture, and circular defects are the form of defects often observed in experiments; We provide the variation of energy during relaxation for different types and sizes of defects, and they are all able to reach a stable equilibrium state after sufficient time of relaxation. It should be noted that the rectangular defects set here are along the armchair direction; the method of setting rectangular defects along the zigzag is the same as here. In general, the structural systems after setting up the defects all show good energy stability, and the potential energy of the system with a large proportion of vacancy atoms is larger.

#### 3.4.1. Rectangular defects

To further investigate the effect of rectangular defects on the mechanical properties of TPDH-graphene, we compared the difference in mechanical properties between rectangular defects (lengths of 10, 15 and 30 Å along the zigzag and armchair directions, respectively, with a width of 10 Å) and the case without considering the

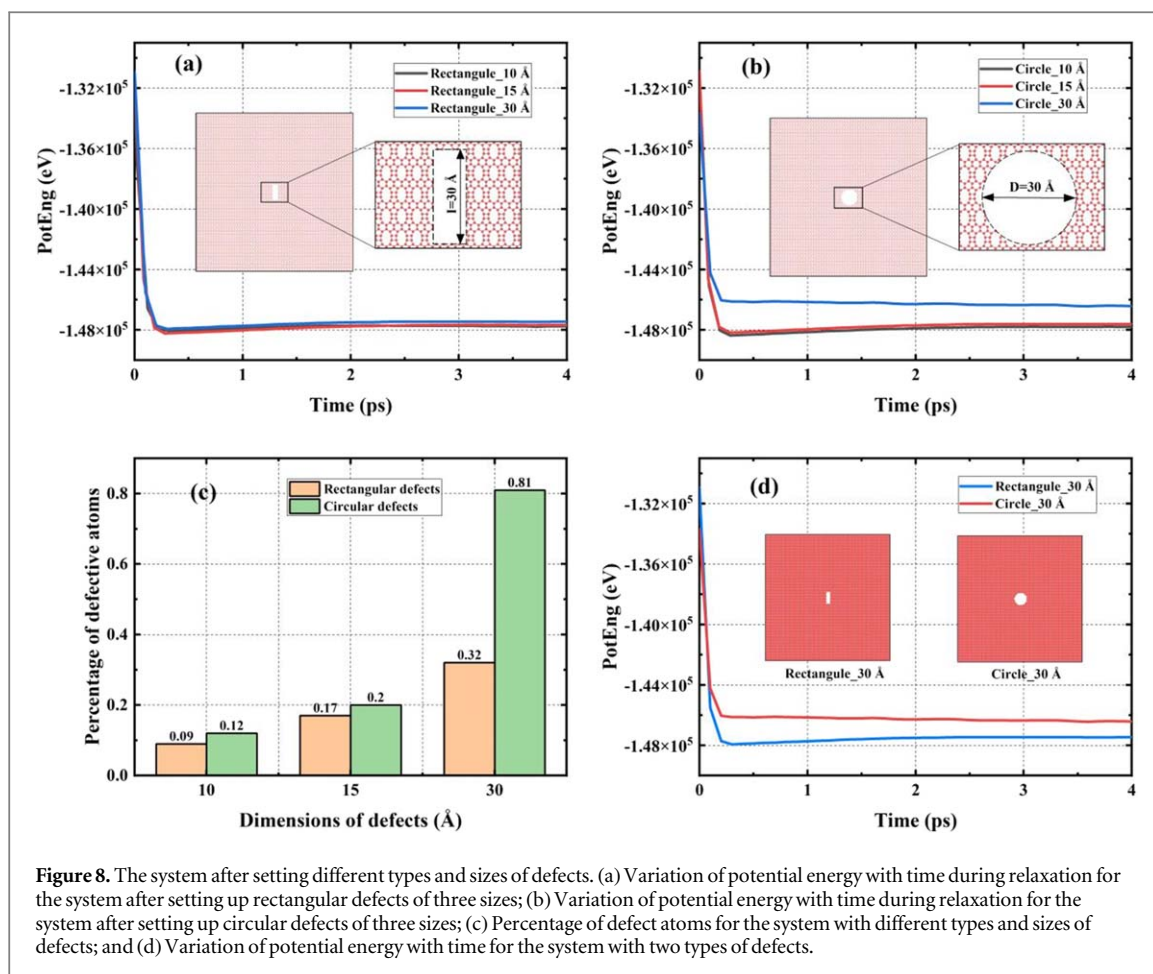


**Figure 8.** The system after setting different types and sizes of defects. (a) Variation of potential energy with time during relaxation for the system after setting up rectangular defects of three sizes; (b) Variation of potential energy with time during relaxation for the system after setting up circular defects of three sizes; (c) Percentage of defect atoms for the system with different types and sizes of defects; and (d) Variation of potential energy with time for the system with two types of defects.

defects. As shown in figure 9(a) for rectangular defects whose length increases along the zigzag direction increasing rectangular defects, with respect to which we do tensile tests in zigzag direction to investigate the effect the length of the defect on its mechanical properties. Similarly, figure 9(b) illustrates the increase of the length of the rectangular defect along the armchair direction.

As shown in figures 10(a)–(d), the mechanical properties of TPDH-graphene weaken with increasing defect length when the rectangular defect length decreases along the zigzag direction, and comparing the mechanical properties of TPDH-graphene without considering defects and considering the case of a rectangular defect with a length of 30 Å, the ultimate stress, ultimate strain, fracture stress, fracture strain and fracture toughness decreased by 58.73%, 58.75%, 58.99%, 58.60% and 80.85%, respectively. As shown in figures 10(e)–(h), the mechanical properties of TPDH-graphene weaken with increasing defect length as the length of the rectangular defect gradually increases along the armchair direction, and the decrease in the stress–strain curves is due to the defects weakening the structural strength of the material. Comparing the mechanical properties of TPDH-graphene without considering defects and considering the case of a rectangular defect with a length of 30 Å in the armchair direction, the ultimate stress, ultimate strain, fracture stress, fracture strain and fracture toughness were reduced by 32.48%, 33.87%, 31.21%, 36.59% and 58.92%, respectively.

As shown in figures 10(e), (d), (g) and (h), we find that TPDH-graphene still exhibits tensile toughness when tensile tests are performed in the armchair direction compared to the zigzag direction; furthermore, the toughness of the added rectangular defects is significantly weakened compared to that of the unadded defects in the TPDH-graphene.

Rectangular defects weaken the mechanical properties of TPDH-graphene to a great extent, and the weakening of the material becomes more significant with the increase of the length of the defects, the reason for which can be well revealed by Griffith's theory [45]. Meanwhile, the setting of defects of the same length causes more significant weakening of the mechanical properties of TPDH-graphene in the zigzag direction, which is due to its own structural differences in different directions.

### 3.4.2. Circular defects

Circular defects are another form of defects different from rectangular defects, and it is also often used to study the effect of defects on the mechanical properties of 2D carbon materials [59]. In order to investigate the effect of

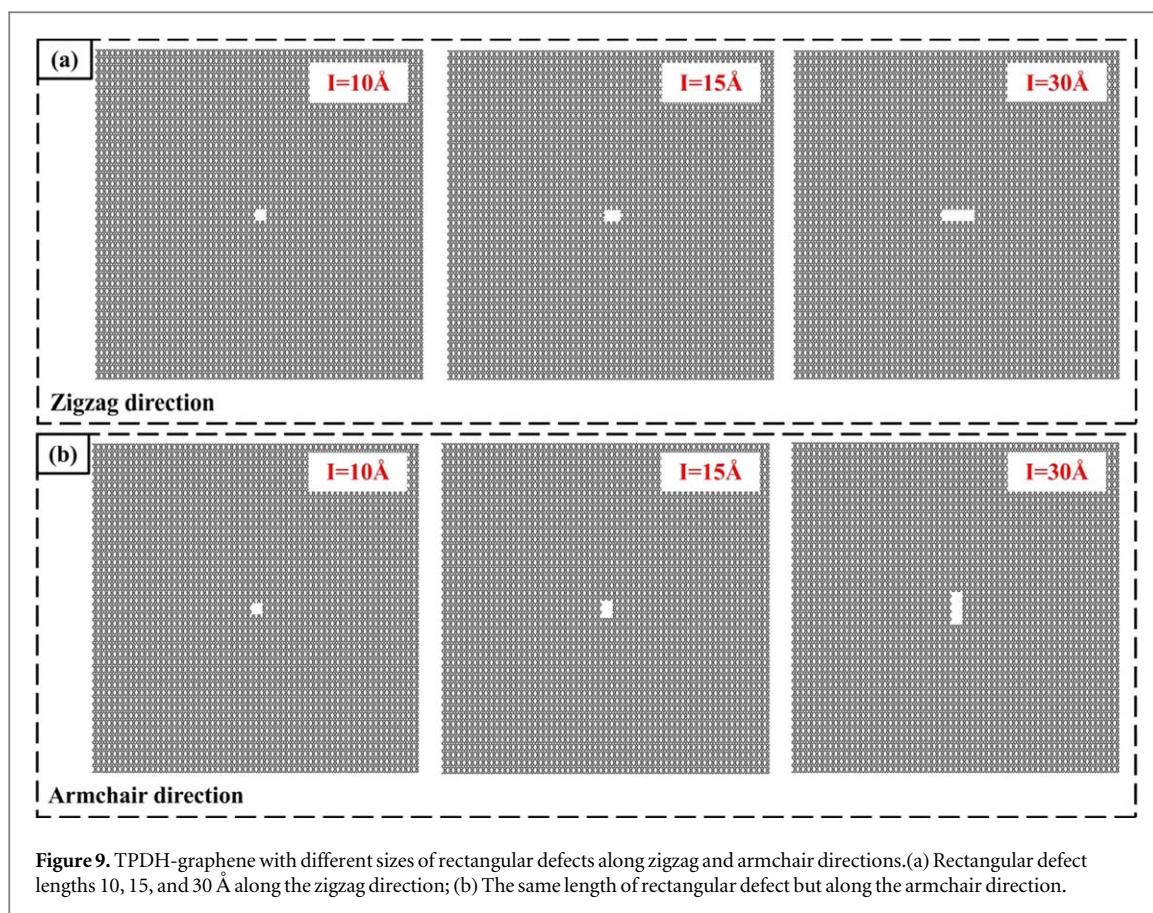


**Figure 9.** TPDH-graphene with different sizes of rectangular defects along zigzag and armchair directions. (a) Rectangular defect lengths 10, 15, and 30 Å along the zigzag direction; (b) The same length of rectangular defect but along the armchair direction.

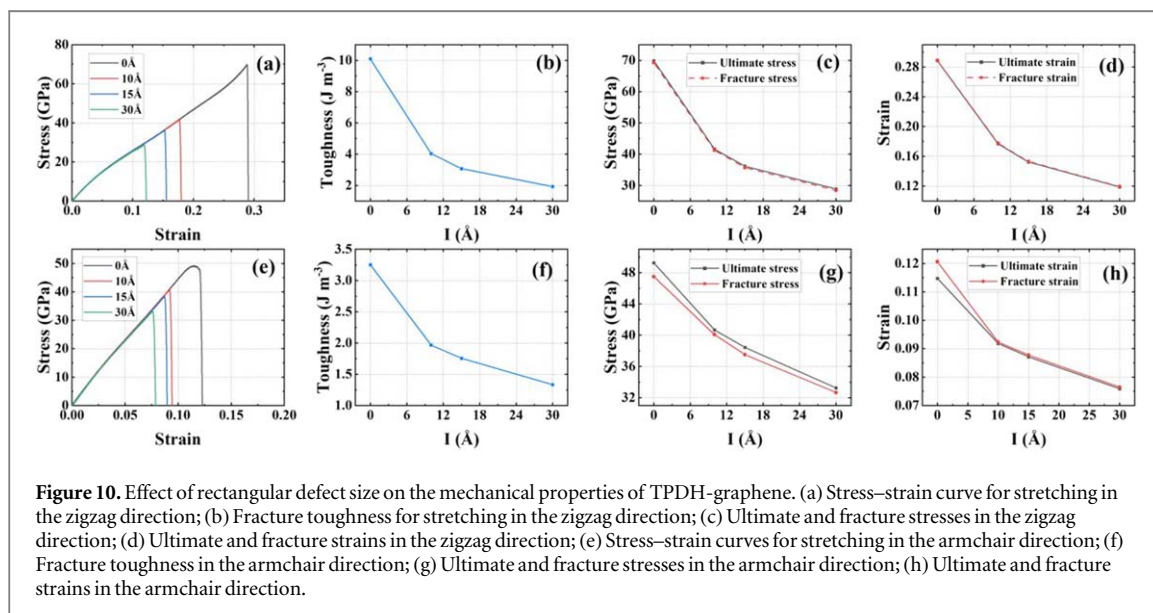


**Figure 10.** Effect of rectangular defect size on the mechanical properties of TPDH-graphene. (a) Stress–strain curve for stretching in the zigzag direction; (b) Fracture toughness for stretching in the zigzag direction; (c) Ultimate and fracture stresses in the zigzag direction; (d) Ultimate and fracture strains in the zigzag direction; (e) Stress–strain curves for stretching in the armchair direction; (f) Fracture toughness in the armchair direction; (g) Ultimate and fracture stresses in the armchair direction; (h) Ultimate and fracture strains in the armchair direction.

circular defect on the mechanical properties of TPDH-graphene, we compared the difference in the mechanical properties of different diameters of circular defect (diameter of 10, 15, and 30 Å, respectively) and without considering the defect, and set up the model of circular defect as shown in figure 11.

As shown in figures 12(a)–(d), tensile tests along the X direction (zigzag) reveal that the mechanical properties of TPDH-graphene weaken as the increase of the diameter of the circular defects increases, and that the damage of the cracks to the original structure of the material leads to a decrease in the stress–strain curve. Comparing the tensile results without considering the defect and considering the circular defect with a diameter of 30 Å, the ultimate stress, ultimate strain, fracture stress, fracture strain and fracture toughness were reduced by 59.85%, 59.58%, 60.71%, 59.47% and 82.65%, respectively. As shown in figures 12(e)–(h), the mechanical

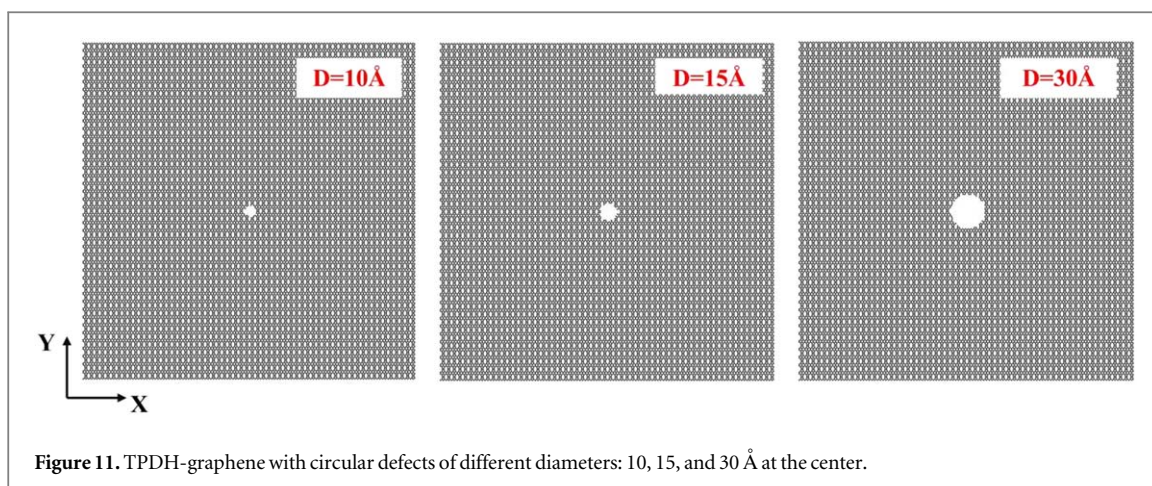


Figure 11. TPDH-graphene with circular defects of different diameters: 10, 15, and 30 Å at the center.

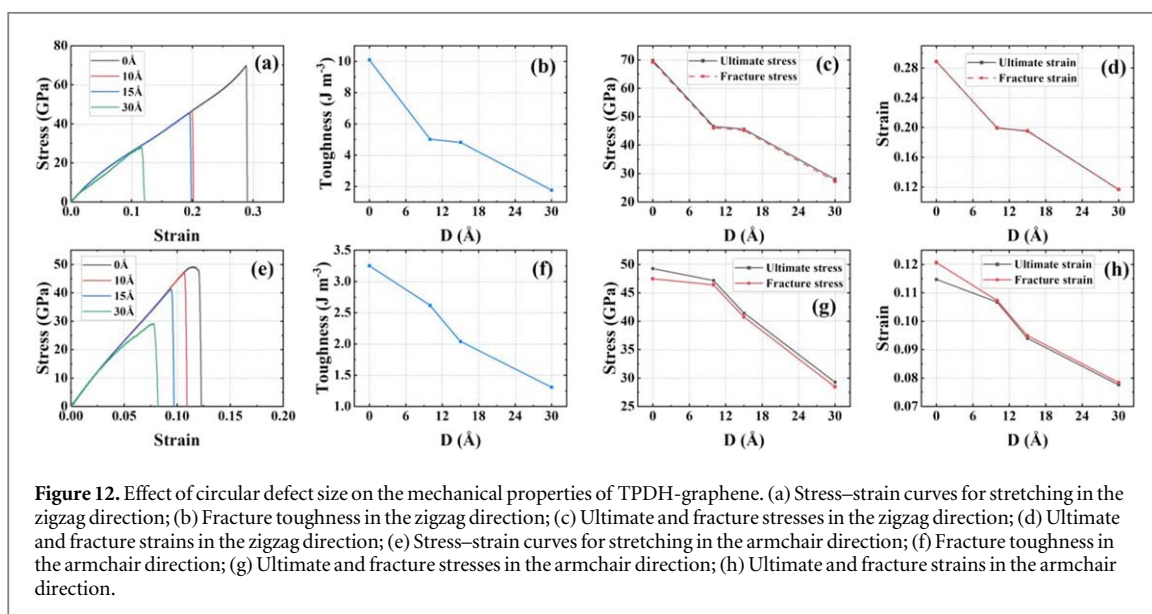


Figure 12. Effect of circular defect size on the mechanical properties of TPDH-graphene. (a) Stress–strain curves for stretching in the zigzag direction; (b) Fracture toughness in the zigzag direction; (c) Ultimate and fracture stresses in the zigzag direction; (d) Ultimate and fracture strains in the zigzag direction; (e) Stress–strain curves for stretching in the armchair direction; (f) Fracture toughness in the armchair direction; (g) Ultimate and fracture stresses in the armchair direction; (h) Ultimate and fracture strains in the armchair direction.

properties of TPDH-graphene weakened with increasing diameter of circular defects when tested in tensile along the Y direction (armchair), similarly comparing its tensile results without defects to those considering circular defects with a diameter of 30 Å, the ultimate stress, ultimate strain, fracture stress, fracture strain and fracture toughness decreased by 40.53%, 32.29%, 40.09%, 34.98% and 56.66% respectively.

As shown in figures 12(c), (d), (g) and (h), the TPDH-graphene with both circular defects and perfect structure added exhibits brittle fracture in the zigzag direction; in the armchair direction it still exhibits a certain degree of tensile toughness, however, the tensile toughness is weakened by the addition of defects. The defects resulted in a localised disruption of the structure of TPDH-graphene. This structural irregularity may make the material more susceptible to fracture when subjected to stress. The reason for this is that there is usually a concentration of stress at the defect, which leads to the stress at the defect exceeding the strength limit of the material, thus triggering brittle fracture.

It can be concluded that circular defects disrupt the intact TPDH-graphene structure and that increasing the diameter of the circular defect reduces the mechanical properties, especially the fracture stress, fracture strain and fracture toughness. Similar to rectangular defects, the increase in diameter of circular defects does not weaken the mechanical properties of TPDH-graphene in the zigzag and armchair directions to the same extent, with the weakening in the zigzag direction being greater than the weakening in the armchair direction, and the explanation for this fact has been given in the section on the study of rectangular defects.

#### 4. Conclusions

In this study, we have used a molecular dynamics approach to comprehensively investigate the effects of strain rates, tensile direction, temperature, and defect size on the mechanical properties of TPDH-graphene;

specifically, the changes in stress–strain curves, ultimate stress, ultimate strain, fracture stress, fracture strain and fracture toughness were observed under different influencing factors. The results show that lower strain rates result in lower fracture stresses and fracture strains; the mechanical properties of TPDH-graphene differ in the zigzag and armchair directions and exhibit significant anisotropy; elevated temperatures for TPDH-graphene will cause the material to soften, which in turn will weaken the mechanical properties of the material; both rectangular and circular defects weaken its mechanical properties to varying degrees, and the degree of weakening is different in the zigzag and armchair directions. Both rectangular and circular defects weaken its mechanical properties to different degrees and in the zigzag and armchair directions, which is related to its own structural differences in the zigzag and armchair directions. TPDH-graphene has a certain tensile toughness along the direction of armchair, and the tensile toughness is weakened by the addition of defects.

The results of this study complement the research on TPDH-graphene, a novel 2D carbon material. Overall, this study provides a reference on the mechanical properties of TPDH-graphene for possible subsequent practical applications in the field of nanoelectronics and highlights the importance of taking into account orientation, temperature and defect size variations.

## Acknowledgment

The authors would like to acknowledge the support provided by the Shenzhen Science and Technology Program (Grant No. KQTD20200820113045081), the National Natural Science Foundation of China (grant No. 12272378), the Strategic Priority Research Program of the Chinese Academy of Sciences (grant No. XDB0620103), and the High-level Innovation Research Institute Program of Guangdong Province (grant No. 2020B0909010003).

## Data availability statement

All data that support the findings of this study are included within the article (and any supplementary files).

## ORCID iDs

Qing Peng  <https://orcid.org/0000-0002-8281-8636>

## References

- [1] Zhang M, Yang H, Li H, Tong L, Su C, Feng K, Wang Q, Yan H and Yin S 2023 Transparent single crystal graphene flexible strain sensor with high sensitivity for wearable human motion monitoring *J. Alloys Compd.* **967** 171724
- [2] Ren S, Rong P and Yu Q 2018 Preparations, properties and applications of graphene in functional devices: a concise review *Ceram. Int.* **44** 11940–55
- [3] Cao Q, Geng X, Wang H, Wang P, Liu A, Lan Y and Peng Q 2018 A review of current development of graphene mechanics *In: Crystals*, (<https://doi.org/10.3390/cryst8090357>)
- [4] Torkaman-Asadi M A and Kouchakzadeh M A 2022 Atomistic simulations of mechanical properties and fracture of graphene: a review *Comput. Mater. Sci.* **210** 111457
- [5] Cao K, Feng S, Han Y, Gao L, Hue Ly T, Xu Z and Lu Y 2020 Elastic straining of free-standing monolayer graphene *Nat. Commun.* **11** 284
- [6] Mazilova T I, Sadanov E V and Mikhailovskij I M 2019 Tensile strength of graphene nanoribbons: an experimental approach *Mater. Lett.* **242** 17–9
- [7] Lee C, Wei X, Kysar J W and Hone J 2008 Measurement of the elastic properties and intrinsic strength of monolayer graphene *Science* **321** 385–8
- [8] Gao Y and Hao P 2009 Mechanical properties of monolayer graphene under tensile and compressive loading *Physica E* **41** 1561–6
- [9] Muhammad I, Hussain F, Khalil R M A, Sattar M A, Mehboob H, Javid M A, Rana A M and Ahmad S A 2019 Anisotropic thermal and mechanical characteristics of graphene: a molecular dynamics study *J. Exp. Theor. Phys.* **128** 259–67
- [10] Jhon Y I, Jhon Y M, Yeom G Y and Jhon M S 2014 Orientation dependence of the fracture behavior of graphene *Carbon* **66** 619–28
- [11] Deng B, Hou J, Zhu H, Liu S, Liu E, Shi Y and Peng Q 2017 The normal-auxeticity mechanical phase transition in graphene *2D Mater.* **4** 021020
- [12] Zhao H and Aluru N R 2010 Temperature and strain-rate dependent fracture strength of graphene *J. Appl. Phys.* **108**
- [13] Gupta K K *et al* (Springer Singapore) 793–804
- [14] Shen L, Shen H-S and Zhang C-L 2010 Temperature-dependent elastic properties of single layer graphene sheets *Mater. Des.* **31** 4445–9
- [15] Dewapriya M A N, Rajapakse R K N D and Phani A S 2014 Atomistic and continuum modelling of temperature-dependent fracture of graphene *Int. J. Fract.* **187** 199–212
- [16] Mortazavi B, Rémond Y, Ahzi S and Toniazzo V 2012 Thickness and chirality effects on tensile behavior of few-layer graphene by molecular dynamics simulations *Comput. Mater. Sci.* **53** 298–302
- [17] Bedi D, Sharma S and Tiwari S K 2022 Effect of chirality and defects on tensile behavior of carbon nanotubes and graphene: Insights from molecular dynamics *Diam. Relat. Mater.* **121** 108769

- [18] Wei Y, Wu J, Yin H, Shi X, Yang R and Dresselhaus M 2012 The nature of strength enhancement and weakening by pentagon–heptagon defects in graphene *Nat. Mater.* **11** 759–63
- [19] Mortazavi B and Ahzi S 2013 Thermal conductivity and tensile response of defective graphene: a molecular dynamics study *Carbon* **63** 460–70
- [20] Ren Y and Cao G 2016 Effect of geometrical defects on the tensile properties of graphene *Carbon* **103** 125–33
- [21] Li H, Zhang H and Cheng X 2017 The effect of temperature, defect and strain rate on the mechanical property of multi-layer graphene: coarse-grained molecular dynamics study *Physica E* **85** 97–102
- [22] Li M, Deng T, Zheng B, Zhang Y, Liao Y and Zhou H 2019 Effect of defects on the mechanical and thermal properties of graphene *Nanomaterials*, (<https://doi.org/10.3390/nano9030347>)
- [23] Yu T, Li J, Yang Z, Li H, Peng Q and Tang H-K 2023 Effects of crack formation on the mechanical properties of bilayer graphene: a comparative analysis *In: Crystals*, (<https://doi.org/10.3390/cryst13040584>)
- [24] Wang X, Che J, Huang W, Linghu J and Hou Z 2023 Mechanism of crack propagation in penta-graphene *Vacuum* **207** 111582
- [25] Ghorbanali S, Zaminpayma E and Mobarakinia H 2023 Miakhs carbon allotropes: three novel two-dimensional carbon allotropes with  $sp^{2+}$   $sp^3$  hybridized network *Comput. Mater. Sci.* **229** 112437
- [26] Wang S, Li J, Zhu X and Wang M 2019 A new two-dimensional semiconducting carbon allotrope: a first-principles study *Carbon* **143** 517–22
- [27] Bhattacharya D and Jana D 2019 First-principles calculation of the electronic and optical properties of a new two-dimensional carbon allotrope: tetra-penta-octagonal graphene *Phys. Chem. Chem. Phys.* **21** 24758–67
- [28] Kilic ME and Lee K-R 2022 Four-penta-graphenes: novel two-dimensional fenestrane-based auxetic nanocarbon allotropes for nanoelectronics and optoelectronics *Carbon* **195** 154–64
- [29] Jiang J-W, Leng J, Li J, Guo Z, Chang T, Guo X and Zhang T 2017 Twin graphene: a novel two-dimensional semiconducting carbon allotrope *Carbon* **118** 370–5
- [30] Bhattacharya D and Jana D 2021 TPDH-graphene: a new two dimensional metallic carbon with NDR behaviour of its one dimensional derivatives *Physica E* **127** 114569
- [31] Oliveira cc, Medina M, Galvao D S and Autreto P A S 2023 Tetra-penta-deca-hexagonal-graphene (TPDH-graphene) hydrogenation patterns: dynamics and electronic structure *Physical Chemistry Chemical Physics: PCCP* **25** 13088–93
- [32] Plimpton S 1995 Fast parallel algorithms for short-range molecular dynamics *J. Comput. Phys.* **117** 1–19
- [33] Stukowski A 2010 Visualization and analysis of atomistic simulation data with OVITO—the open visualization tool *Model. Simul. Mater. Sci. Eng.* **18** 015012
- [34] Winczewski S, Shaheen M Y and Rybicki J 2018 Interatomic potential suitable for the modeling of penta-graphene: molecular statics/ molecular dynamics studies *Carbon* **126** 165–75
- [35] Han C C, He P F and Zheng B L 2012 *Numerical Simulation of the Effect of Crack on the Tensile Mechanical Properties of Graphene*. 2012 *Third Int. Conf. on Digital Manufacturing & Automation* 562–5
- [36] Budarapu P R, Javvaji B, Sutrarak V K, Roy Mahapatra D, Zi G and Rabczuk T 2015 Crack propagation in graphene *J. Appl. Phys.* **118** 064307
- [37] Sutrarak V K, Javvaji B and Budarapu P R 2021 Fracture strength and fracture toughness of graphene: MD simulations *Appl. Phys. A* **127** 949
- [38] Eftekhari S A, Toghraie D, Hekmatifar M and Sabetvand R 2021 Mechanical and thermal stability of armchair and zig-zag carbon sheets using classical MD simulation with Tersoff potential *Physica E* **133** 114789
- [39] Dewapriya M A N, Meguid S A and Rajapakse R K N D 2018 Atomistic modelling of crack-inclusion interaction in graphene *Eng. Fract. Mech.* **195** 92–103
- [40] Bu H, Chen Y, Zou M, Yi H, Bi K and Ni Z 2009 Atomistic simulations of mechanical properties of graphene nanoribbons *Phys. Lett. A* **373** 3359–62
- [41] Ni Z, Bu H, Zou M, Yi H, Bi K and Chen Y 2010 Anisotropic mechanical properties of graphene sheets from molecular dynamics *Physica B* **405** 1301–6
- [42] Mortazavi B, Rajabpour A, Ahzi S, Rémond Y and Mehdi Vaez Allaei S 2012 Nitrogen doping and curvature effects on thermal conductivity of graphene: a non-equilibrium molecular dynamics study *Solid State Commun.* **152** 261–4
- [43] Rajasekaran G, Kumar R and Parashar A 2016 Tersoff potential with improved accuracy for simulating graphene in molecular dynamics environment *Mater. Res. Express* **3** 035011
- [44] Tersoff J 1994 Chemical order in amorphous silicon carbide *Phys. Rev. B* **49** 16349–52
- [45] Griffith A A 1920 The phenomena of rupture and flow in solids *Philosophical Transactions of The Royal Society A Mathematical Physical and Engineering Sciences* **A221** 163–98
- [46] Rakib T, Mojumder S, Das S, Saha S and Motalab M 2017 Graphene and its elemental analogue: a molecular dynamics view of fracture phenomenon *Physica B* **515** 67–74
- [47] Gamboa-Suárez A, Seuret-Hernández H Y and Leyssale J-M 2022 Mechanical properties of pristine and nanocrystalline graphene up to ultra-high temperatures *Carbon Trends* **9** 100197
- [48] Bedi D, Sharma S, Tiwari S K and Ajori S 2022 Effect of defects and boundary conditions on the vibrational behavior of carbon nanotube and graphene: a molecular dynamics perspective *Diam. Relat. Mater.* **126** 109052
- [49] Zhang Y-Y, Pei Q-X, Mai Y-W and Gu Y-T 2014 Temperature and strain-rate dependent fracture strength of graphynes *J. Phys. D: Appl. Phys.* **47** 425301
- [50] Rida A, Micoulaut M, Rouhaud E and Makke A 2020 Understanding the strain rate sensitivity of nanocrystalline copper using molecular dynamics simulations *Comput. Mater. Sci.* **172** 109294
- [51] Chen M Q, Quek S S, Sha Z D, Chiu C H, Pei Q X and Zhang Y W 2015 Effects of grain size, temperature and strain rate on the mechanical properties of polycrystalline graphene—a molecular dynamics study *Carbon* **85** 135–46
- [52] Tanhadoust A, Jahanshahi M and Khoei A R 2022 Temperature-dependent multiscale modeling of graphene sheet under finite deformation *Diam. Relat. Mater.* **129** 109334
- [53] Ajori S and Eftekhari A R 2022 Mechanical properties and fracture analysis of defective penta-graphene under temperature variation: insight from molecular dynamics *Diam. Relat. Mater.* **124** 108956
- [54] Ansari R, Motavalli B, Montazeri A and Ajori S 2011 Fracture analysis of monolayer graphene sheets with double vacancy defects via MD simulation *Solid State Commun.* **151** 1141–6
- [55] Zhang S, Wang Z and Wang X 2024 Effect of defects on mechanical properties of  $\Psi$ -graphene nanotubes via molecular dynamics simulations *Physica B* **674** 415461

- [56] Kumar Y, Sahoo S and Chakraborty A K 2021 Mechanical properties of graphene, defective graphene, multilayer graphene and SiC-graphene composites: a molecular dynamics study *Physica B* **620** 413250
- [57] Zheng B and Gu G X 2019 Tuning the graphene mechanical anisotropy via defect engineering *Carbon* **155** 697–705
- [58] Farzin A, Etemadi M, Mehran S and Rouhi S 2023 Investigating the mechanical properties of perfect and defective  $\Psi$ -graphene: a molecular dynamics simulation *Materials Today Communications* **37** 106908
- [59] Samadian M, Ajri M, Azizi A and Hemmatpour-Khotbesara M A 2023 Investigating the pinhole effect on the mechanical properties of biphenylene *Appl. Phys. A* **129** 826